Springer

KSME

Journal of Mechanical Science and Technology 30 (7) (2016) 3203~3218
www.springerlink.com/content/1738-494x(Print)/1976-3824(Online)
DOI 10.1007/s12206-016-0629-0

Influence of slip velocity in Herschel-Bulkley fluid flow between parallel plates - A mathematical study †

D. S. Sankar[1] and Usik Lee[2,*]

[1]*Engineering Mathematics Unit, Faculty of Engineering, Universiti Teknologi Brunei, Gadong BE1410, Bandar Seri Begawan, Brunei Darussalam*
[2]*Department of Mechanical Engineering, Inha University, Inha-Ro 100, 253 Yonghyun-Dong, Nam-Gu, Incheon 402-751, Korea*

(Manuscript Received October 31, 2015; Revised March 6, 2016; Accepted March 25, 2016)

Abstract

This theoretical study investigates three types of basic flows of viscous incompressible Herschel-Bulkley fluid such as (i) plane Couette flow, (ii) Poiseuille flow and (iii) generalized Couette flow with slip velocity at the boundary. The analytic solutions to the nonlinear boundary value problems have been obtained. The effects of various physical parameters on the velocity, flow rate, wall shear stress and frictional resistance to flow are analyzed through appropriate graphs. It is observed that in plane Poiseuille flow and generalized Couette flow, the velocity and flow rate of the fluid increase considerably with the increase of the slip parameter, power law index, pressure gradient. The fluid velocity is significantly higher in plane Poiseuille flow than in plane Couette flow. The wall shear stress and frictional resistance to flow decrease considerably with the increase of the power law index and increase significantly with the increase of the yield stress of the fluid. The wall shear stress and frictional resistance to flow are considerably higher in plane Poiseuille flow than in generalized Couette flow.

Keywords: Herschel-Bulkley fluid; Plane Couette flow; Poiseuille flow; Generalized Couette flow; Slip velocity

1. Introduction

Recently, non-Newtonian fluid flows attracted several researchers due to its growing applications in various fields of science and engineering, such as bio-fluid mechanics, biomedical engineering, chemical engineering, food processing technology, polymer extrusion processes, drilling operations, metallurgy etc [1]. Herschel-Bulkley (H-B) fluid is classified as non-Newtonian fluid with yield stress, since the relationship between the shear stress and rate of strain of this fluid model is nonlinear [2, 3]. Due to its distinct physical properties, it finds applications in the manufacturing of bioengineering products, paints, synthetic lubricants and also in the biological fluid flows such as blood, synovial fluids etc [4-6].

The studies on the incompressible fluid flow with slip velocity at the boundary of the flow region was proposed by Navier [7] in 1823 and he propounded that the tangential velocity of the fluid at any point on the surface of the solid boundary is proportional to the tangential stress acting at that point. The contributions of Basset [8] and O'Neil et al. [9] are some sample studies for the existence of the slip velocity at the boundary of the flow region. It is well understood that in most of the flow problems studied at the micro scale, the assumption of no-slip velocity at the boundary is true only if the surface of the boundary is very rough, since the no-slip velocity conditions in this case cannot not derived from the first principle [10, 11]. Goldstein [12] and Batchelor [13] reported that the use of no-slip velocity at the boundary stems from the necessity that the theoretical predictions need to agree with the experimental observations. But, if the surface of the boundary is smooth, then the usual assumption of no-slip velocity at the boundary is not valid, indeed the fluid slips at the smooth boundary as this is more evident from the studies of Lauga et al. [10], Denn [14], Potente et al. [15], Mitsoulis et al. [16]. Denn [14] propounded that in molecular studies such as in polymer melts and polymer extrusion process, at the boundary the slip effects are found at the macro scale which leads to flow instabilities.

The aforementioned wealthy background on the slip velocity at the boundary of fluid flow attracted the attention of several researchers to do further investigations in this field with applications to various disciplines of engineering and technology [17-20]. The analytical solutions of shear flow problems with slip velocity at the boundary play a major role not only in solving the relevant industrial problems, but also to understand the complexity of many flow problems. Indeed there are many analytical solutions available in the literature for slip

*Corresponding author. Tel.: +82 32 860 7318, Fax.: +82 32 866 1434
E-mail address: ulee@inha.ac.kr
† Recommended by Associate Editor Do Hyung Lee

shear flow problems and of these, some of them are very trivial and others involve more complex rheological parameters [21-26]. Although the simple shear flow solutions seem to be trivial, they are very useful for the better understanding of more complex solutions and even these solutions lead to novel methods to solve advanced level problems [27-29].

Wu et al. [30] obtained analytical solutions to the pressure driven unsteady flow of Newtonian fluid in micro-tubes with slip velocity as defined by Navier [7]. In an analytical study on the flow through a pipe, Mathews and Hill [24] used the sip boundary conditions proposed by Thompson and Troian [31], while Yang ang Zhau [23] used the slip velocity condition of Navier [7] in their theoretical studies to the squeeze flow in a pipe. Hakeem et al. [32] investigated the effects of slip velocity in the peristaltic motion of power law fluid through an inclined tube. Chen and Zhu [33] performed analytical studies on the Couette-Poiseuille flow of Bingham fluid between two parallel porous plates. Abelman et al. [34] obtained numerical solutions for their computational study on the steady Couette flow of thermodynamic third grad fluid through porous medium, using rotating frame of reference. Noor et al. [35] investigated the effects of slip velocity in the mixed convection stagnation flow of micropolar nanofluid along a vertically stetching surface. Devakar and Ramesh [36] analytically investigated the Couette flow, Poiseuille flow and generalized Couette flow of Casson fluid between parallel plates.

The (i) plane Couette flow (ii) plane Poiseuille flow and (iii) generalized Couette flow of viscous incompressible fluid are some of the simple shear flows in the axial (horizontal) direction and although the analytical solutions of these flows are simple, these solutions are the building blocks for the easy understanding of more complex fluid flows. Since the Herschel-Bulkley (H-B) fluid model has one more parameter namely the power law index n than the Casson fluid model, it is hoped that the use of H-B fluid model rather than Casson fluid model in these types of flows would yield more information on flow characteristics. As mentioned by Chaturani [37] and Tu and Deville [2], Casson fluid model can be used for flow at moderate shear rates, whereas, the H-B fluid model can still be used at low shear rates. Hence, it is appropriate to model the incompressible fluid used in these kinds of flow as H-B fluid model rather than Casson fluid model.

The mathematical modeling of H-B fluid for the (i) plane Couette flow, (ii) plane Poiseuille flow and (iii) generalized Couette flow between parallel plates was not studied by any one so far, to the knowledge of the author. Hence, in this mathematical analysis, we investigate the steady, laminar and fully developed flow of viscous incompressible fluid between parallel plates, considering the flow to be (i) plane Couette flow, (ii) plane Poiseuille flow and (iii) generalized Couette flow, the flowing fluid is modeled as H-B fluid model. It is noted that for particular values of the parameters n and τ_y, the H-B fluid model reduces to Bingham fluid model, power law fluid model and Newtonian fluid model which are widely used in the modeling of industrial engineering problems. When n = 1, H-B fluid model reduces to Bingham fluid model, when τ_y = 0, it reduces to the power law index and when n = 1 and τ_y = 0, it reduces to Newtonian fluid model. When n < 1, the H-B fluid model behaves as shear thinning fluid and when n < 1, it exhibits the character of shear thickening fluid. Since the wall shear stress and frictional resistance to flow are important flow measurements which are widely used to analyze the flow patterns and also in the design of flow channels in industrial engineering. In addition to the studies on the effects of slip velocity on the velocity distribution and volumetric flow rate, the present study also discusses the effects of slip velocity on the wall shear stress and frictional resistance to flow which are not studied by Devakar and Ramesh [35]. Hence, it is felt that the present study will have more scope than the earlier studies in applications point of view. The layout of the paper is given below:

In Sec. 2, the three types of flows such as (i) plane Couette flow, (ii) plane Poiseuille flow and (iii) generalized Couette flow are mathematically formulated and then the analytical solutions to velocity distribution, flow rate, frictional resistance to flow and wall shear stress are obtained for each of the flow considered. The variation of the aforementioned flow quantities with yield stress, slip parameter, power law index and pressure gradient are discussed through appropriate graphs in Sec. 3. The main findings of this investigation are summarized in the conclusion Sec. 4.

2. Mathematical formulation and solution method

2.1 Basic governing equations

For the laminar and fully developed flow of viscous incompressible fluid, the equations of continuity and momentum reduce to the following form:

$$\nabla \cdot \vec{q} = 0 \tag{1}$$

$$\bar{\rho}\frac{D\bar{u}_i}{D\bar{t}} = \frac{\partial}{\partial \bar{x}_j}\left(\bar{\sigma}_{ij}\right), \quad i = 1,2,3 \tag{2}$$

where $\vec{q} = \left(\bar{u}_1, \bar{u}_2, \bar{u}_3\right)$ is the velocity vector, $\bar{\rho}$ is the fluid's density, D/Dt is the material derivative; $\left(\bar{x}_1, \bar{x}_2, \bar{x}_3\right)$ is the Cartesian coordinate system; σ_{ij} is the Cauchy's stress tensor. The modified constitutive equation (in the tensor form) of the generalized Newtonian fluid model which establishes the relationship between the stress and the rate of strain is given below [38, 39]:

$$\bar{\sigma}_{ij} = -\bar{p}\delta_{ij} + 2\bar{\mu}(\bar{J}_2)\bar{V}_{ij} \tag{3}$$

where $\bar{p}$ is the pressure; $\bar{J}_2$ and $\bar{V}_{ij}$ are the second invariant of the stress tensor and deformation tensor respectively; δ_{ij} is the Kronecker delta; $\bar{\mu}(\bar{J}_2)$ is the variable viscosity of the generalized Newtonian fluid. Herschel-Bulkley (H-B) fluid is a non-Newtonian (generalized Newtonian) fluid with yield stress and for this fluid, the viscosity coefficient $\bar{\mu}(\bar{J}_2)$ is defined as below:

$$\bar{\mu}(\bar{J}_2) = \bar{K}\left|\bar{J}_2\right|^{n-1} + \frac{\bar{\tau}_y}{\left|\bar{J}_2\right|} \tag{4}$$

where $\bar{K} = \sqrt[n]{\bar{\mu}_H}$; $\bar{\mu}_H$ and $\bar{\tau}_y$ are the H-B fluid's coefficient of viscosity and yield stress respectively; n is the power law index and

$$\bar{J}_2 = \frac{1}{2}\bar{V}_{ij}\bar{V}_{ij} = \frac{1}{2}\left[\bar{V}_{11}^2 + \bar{V}_{22}^2 + \bar{V}_{33}^2 + 2\left(\bar{V}_{12}^2 + \bar{V}_{13}^2 + \bar{V}_{23}^2\right)\right] \tag{5}$$

$$\bar{V}_{ij} = \frac{1}{2}\left(\frac{\partial \bar{u}_i}{\partial \bar{x}_j} + \frac{\partial \bar{u}_j}{\partial \bar{x}_i}\right), \text{ for } i, j = 1,2,3. \tag{6}$$

For the uni-directional steady, laminar and slow flow of viscous incompressible fluid in the horizontal direction in a channel between parallel flat plates, let us use Cartesian coordinate system $(\bar{x}_1, \bar{x}_2, \bar{x}_3) = (\bar{x}, \bar{y}, \bar{z})$ to analyze the flow. We denote the velocity vector by $\vec{q} = (\bar{u}_1, \bar{u}_2, \bar{u}_3) = (\bar{u}, 0, 0)$. For this flow, the aforesaid governing equations of motion reduce to the following equation:

$$\frac{d}{d\bar{y}}\left[\left\{\bar{K}\left(\frac{d\bar{u}}{d\bar{y}}\right)^{\frac{1}{n}-1} + \frac{\bar{\tau}_y}{\left(\frac{d\bar{u}}{d\bar{y}}\right)}\right\}\left(\frac{d\bar{u}}{d\bar{y}}\right)\right] - \frac{d\bar{p}}{d\bar{x}} = 0. \tag{7}$$

2.2 Plane Couette flow

Let us consider the steady, laminar and fully developed flow of viscous incompressible H-B fluid in a channel between two infinitely long horizontal parallel plates which are at distant 2*h*. The pressure gradient between the plates is taken as zero, i.e. the pressure $\bar{p}$ between the plates is assumed as constant. The lower plate $\bar{y} = -\bar{h}$ is held fixed, while the upper plate $\bar{y} = \bar{h}$ is jerked suddenly with constant velocity $\bar{U}$ in the horizontal direction. The fluid flow in the channel is in the $\bar{x}$ direction and is due to the movement of the upper plate. This kind of flow is known as plane Couette flow. The geometry of this flow is shown in Fig. 1(a). Assume that the relative velocity between the plate and fluid is proportional to the plate's shear rate and thus, the governing equation of motion Eq. (7) reduces to

$$\frac{d}{d\bar{y}}\left[\left\{\bar{K}\left(\frac{d\bar{u}}{d\bar{y}}\right)^{\frac{1}{n}-1} + \bar{\tau}_y\left(\frac{d\bar{y}}{d\bar{u}}\right)\right\}\left(\frac{d\bar{u}}{d\bar{y}}\right)\right] = 0. \tag{8}$$

The slip boundary conditions of this flow are

$$\bar{u}\left(-\bar{h}\right) - \bar{\beta}\left[\left\{\bar{K}\left(\frac{d\bar{u}}{d\bar{y}}\right)^{\frac{1}{n}-1} + \bar{\tau}_y\left(\frac{d\bar{y}}{d\bar{u}}\right)\right\}\left(\frac{d\bar{u}}{d\bar{y}}\right)\right]_{\bar{y}=-\bar{h}} = 0 \tag{9a}$$

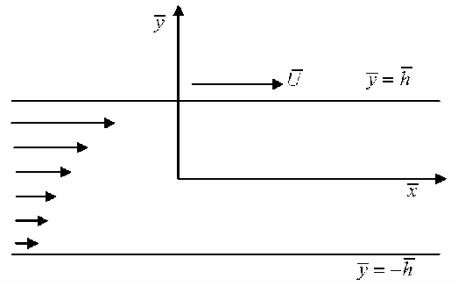

(a) Plane Couette flow

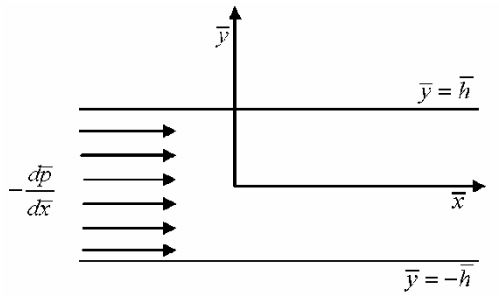

(b) Plane Poiseuille flow

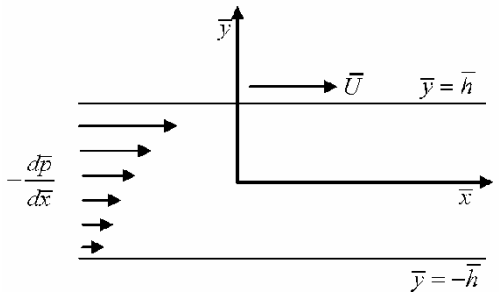

(c) Generalized Couette flow

Fig. 1. Pictorial description of flow geometries between parallel plates.

$$\bar{u}\left(\bar{h}\right) + \bar{\beta}\left[\left\{\bar{K}\left(\frac{d\bar{u}}{d\bar{y}}\right)^{\frac{1}{n}-1} + \bar{\tau}_y\left(\frac{d\bar{y}}{d\bar{u}}\right)\right\}\left(\frac{d\bar{u}}{d\bar{y}}\right)\right]_{\bar{y}=\bar{h}} = \bar{U} \tag{9b}$$

where $\bar{\beta}$ is the slip parameter. Let us introduce the following non-dimensional variables:

$$y = \frac{\bar{y}}{\bar{h}};\ u = \frac{\bar{u}}{\bar{U}};\ \tau_y = \frac{\sqrt[n]{\bar{h}}\,\bar{\tau}_y}{\bar{K}\sqrt[n]{\bar{U}}};\ \gamma = \frac{\bar{K}\sqrt[n]{\bar{U}}\,\bar{\beta}}{\bar{U}\sqrt[n]{\bar{h}}}. \tag{10}$$

Using the non-dimensional variables Eq. (10) into Eq. (8), we get the dimensionless form of the equation of motion as

$$\frac{d}{dy}\left[\left(\frac{du}{dy}\right)^{\frac{1}{n}} + \tau_y\right] = 0. \tag{11}$$

The non-dimensional form of the boundary conditions Eqs. (9a) and (9b) are given below:

$$u(-1)-\gamma\left[\left(\frac{du}{dy}\right)^{\frac{1}{n}}+\tau_y\right]_{y=-1}=0 \tag{12a}$$

$$u(1)+\gamma\left[\left(\frac{du}{dy}\right)^{\frac{1}{n}}+\tau_y\right]_{y=1}=1\,. \tag{12b}$$

Integration of Eq. (11) yields

$$\left(\frac{du}{dy}\right)^{\frac{1}{n}}+\tau_y=A \tag{13}$$

where A is the constant of integration to be determined. Using Eq. (13) in Eqs. (12a) and (12b), we obtain

$$u(-1)=\gamma A \tag{14a}$$

$$u(1)=1-\gamma A\,. \tag{14b}$$

From Eq. (13), one can obtain the expression for fluid velocity as

$$u(y)=Ry+B \tag{15}$$

where

$$R=\left(A-\tau_y\right)^n \tag{16}$$

and B is the constant of integration to be determined. Using the boundary conditions Eqs. (14a) and (14b) in Eq. (15), we obtain

$$R=\frac{1}{2}(1-2\gamma A)$$
$$B=\frac{1}{2}\,. \tag{17}$$

Substitution of R and B values in Eq. (15) yields

$$u(y)=\frac{1}{2}\left[1+(1-2\gamma A)y\right]. \tag{18}$$

From Eqs. (16) and (17), one can get

$$2\left(A-\tau_y\right)^n+2\gamma A-1=0\,. \tag{19}$$

Eq. (19) is a non-linear equation for the unknown A. For a given set of values of τ_H and γ, Eq. (19) can be solved by applying Newton-Raphson method. The non-dimensional flow rate is obtained with the help of Eq. (18) as below:

$$Q=\int_{-1}^{1}u(y)\,dy=1\,. \tag{20}$$

2.3 Plane Poiseuille flow

Consider the steady, laminar and fully developed flow of viscous incompressible H-B fluid through a channel which is bounded by two infinitely long horizontal parallel plates which are at distant $2h$ and are at rest. It is assumed that the fluid flow is due to the applied constant pressure gradient in the x direction. This kind of flow is generally called as plane Poiseuille flow. The geometry of this flow is depicted in Fig. 1(b). To this flow conditions, the governing equation of motion Eq. (7) remains unchanged and is restated below:

$$\frac{d}{d\bar{y}}\left[\left\{\bar{K}\left(\frac{d\bar{u}}{d\bar{y}}\right)^{\frac{1}{n}-1}+\bar{\tau}_y\left(\frac{d\bar{y}}{d\bar{u}}\right)\right\}\left(\frac{d\bar{u}}{d\bar{y}}\right)\right]-\frac{d\bar{p}}{d\bar{x}}=0\,. \tag{21}$$

For this flow, the slip boundary conditions are

$$\bar{u}\left(-\bar{h}\right)-\bar{\beta}\left[\left\{\bar{K}\left(\frac{d\bar{u}}{d\bar{y}}\right)^{\frac{1}{n}-1}+\bar{\tau}_y\left(\frac{d\bar{y}}{d\bar{u}}\right)\right\}\left(\frac{d\bar{u}}{d\bar{y}}\right)\right]_{\bar{y}=-\bar{h}}=0 \tag{22a}$$

$$\bar{u}\left(\bar{h}\right)+\bar{\beta}\left[\left\{\bar{K}\left(\frac{d\bar{u}}{d\bar{y}}\right)^{\frac{1}{n}-1}+\bar{\tau}_y\left(\frac{d\bar{y}}{d\bar{u}}\right)\right\}\left(\frac{d\bar{u}}{d\bar{y}}\right)\right]_{\bar{y}=\bar{h}}=0 \tag{22b}$$

where β is the slip parameter. Let us introduce the following dimensionless variables (the non-dimensional variables that are defined in Eq. (10) are used here too):

$$y=\frac{\bar{y}}{\bar{h}};\ u=\frac{\bar{u}}{\bar{U}};\ \tau_y=\frac{\sqrt[n]{\bar{h}}\,\bar{\tau}_y}{\bar{K}\sqrt[n]{\bar{U}}};\ \gamma=\frac{\bar{K}\sqrt[n]{\bar{U}}\,\bar{\beta}}{\bar{U}\sqrt[n]{\bar{h}}};$$
$$x=\frac{\bar{x}}{\bar{h}};\ p=\frac{\sqrt[n]{\bar{h}}\,\bar{p}}{\bar{K}\sqrt[n]{\bar{U}}}\,. \tag{23}$$

The non-dimensional form of the governing equation of motion Eq. (21) and the boundary conditions Eqs. (22a) and (22b) are obtained as below respectively:

$$\frac{d}{dy}\left[\left(\frac{du}{dy}\right)^{\frac{1}{n}}+\tau_y\right]=-G \tag{24}$$

$$u(-1)-\gamma\left[\left(\frac{du}{dy}\right)^{\frac{1}{n}}+\tau_y\right]_{y=-1}=0 \tag{25a}$$

$$u(1)+\gamma\left[\left(\frac{du}{dy}\right)^{\frac{1}{n}}+\tau_H\right]_{y=1}=0 \tag{25b}$$

where $G=-dp/dx$. Integrating Eq. (24), one can get

$$\left(\frac{du}{dy}\right)^{\frac{1}{n}} + \tau_y = -Gy + C \tag{26}$$

where C is a constant of integration to be determined. The use of Eq. (26) simplifies the boundary conditions Eqs. (25a) and (25b) to the following form respectively:

$$u(-1) = \gamma(G + C) \tag{27a}$$

$$u(1) = \gamma(G - C). \tag{27b}$$

Simplifying Eq. (26) and then integrating it, we obtain

$$u(y) = -\frac{1}{G(n+1)}\left(C - Gy - \tau_y\right)^{n+1} + D \tag{28}$$

where D is the constant of integration to be determined. Applying the boundary conditions Eqs. (27a) and (27b) in Eq. (28), one can get

$$\left(C + G - \tau_y\right)^{n+1} + (n+1)G\gamma(G + C) - (n+1)GD = 0, \tag{29a}$$

$$\left(C - G - \tau_y\right)^{n+1} + (n+1)G\gamma(G - C) - (n+1)GD = 0. \tag{29b}$$

From Eqs. (29a) and (29b), we obtain the following nonlinear algebraic equation in the unknown C.

$$\left(C - G - \tau_y\right)^{n+1} + (n+1)G\gamma(G - C) - (n+1)GD = 0. \tag{30}$$

For a given set of values of the parameters τ_y, γ, n and G, Eq. (30) can be solved numerically, using the Newton-Raphson method. The non-dimensional flow rate per unit width of the plates is obtained with the help of Eq. (28) as below:

$$\begin{aligned} Q &= \int_{-1}^{1} u(y)\, dy \\ &= \frac{\left\{C - G - \tau_y\right\}^{n+2} - \left\{C + G - \tau_y\right\}^{n+2}}{G^2(n+1)(n+2)} + 2D. \end{aligned} \tag{31}$$

The skin friction or wall shear stress at the lower wall (plate) and upper wall (plate) are defined respectively as

$$\tau_{LW} = \tau\big|_{y=-1} = \left\{\left(\frac{du}{dy}\right)^{1/n}\right\}_{y=-1} + \tau_y = C + G \tag{32a}$$

$$\tau_{UW} = \tau\big|_{y=1} = \left\{\left(\frac{du}{dy}\right)^{1/n}\right\}_{y=1} + \tau_y = C - G. \tag{32b}$$

Note that the subscripts LW and UW in Eqs. (32a) and (32b) denote the lower wall and upper wall, respectively. The frictional resistance to flow is defined as

$$\Lambda = G / Q. \tag{33}$$

2.4 Generalized Couette flow

Let us consider again the steady, laminar, fully developed flow of viscous incompressible H-B fluid between two infinitely long horizontal parallel plates that are at distant $2h$. This flow is similar to the plane Couette flow, but, a constant pressure gradient is also applied in the x direction. This kind of flow is called as generalized plane Couette flow. The geometry of this flow is depicted in Fig. 1(c). For the generalized plane Couette flow, the governing equation of motion Eq. (7) remains the same and is restated below:

$$\frac{d}{d\bar{y}}\left[\left\{\bar{K}\left(\frac{d\bar{u}}{d\bar{y}}\right)^{\frac{1}{n}-1} + \bar{\tau}_y\left(\frac{d\bar{y}}{d\bar{u}}\right)\right\}\left(\frac{d\bar{u}}{d\bar{y}}\right)\right] - \frac{d\bar{p}}{d\bar{x}} = 0. \tag{34}$$

The slip boundary conditions of this flow are

$$\bar{u}\left(-\bar{h}\right) - \bar{\beta}\left[\left\{\bar{K}\left(\frac{d\bar{u}}{d\bar{y}}\right)^{\frac{1}{n}-1} + \bar{\tau}_y\left(\frac{d\bar{y}}{d\bar{u}}\right)\right\}\left(\frac{d\bar{u}}{d\bar{y}}\right)\right]_{\bar{y}=-\bar{h}} = 0 \tag{35a}$$

$$\bar{u}\left(\bar{h}\right) + \bar{\beta}\left[\left\{\bar{K}\left(\frac{d\bar{u}}{d\bar{y}}\right)^{\frac{1}{n}-1} + \bar{\tau}_y\left(\frac{d\bar{y}}{d\bar{u}}\right)\right\}\left(\frac{d\bar{u}}{d\bar{y}}\right)\right]_{\bar{y}=\bar{h}} = \bar{U} \tag{35b}$$

where β is the slip parameter. The dimensionless variables defined in Eq. (23) are used to obtain the non-dimensional form of Eqs. (34) and (35) as below, respectively:

$$\frac{d}{dy}\left[\left(\frac{du}{dy}\right)^{1/n} + \tau_y\right] = -G \tag{36}$$

$$u(-1) - \gamma\left[\left(\frac{du}{dy}\right)^{1/n} + \tau_H\right]_{y=-1} = 0 \tag{37a}$$

$$u(1) + \gamma\left[\left(\frac{du}{dy}\right)^{1/n} + \tau_y\right]_{y=1} = 1 \tag{37b}$$

where $G = -dp/dx$. Integrating Eq. (36), one can obtain

$$\left(\frac{du}{dy}\right)^{1/n} + \tau_y = -Gy + E \tag{38}$$

where E is a constant of integration to be determined. Applying Eq. (38) in the boundary conditions Eqs. (37a) and (37b), one can obtain

$$u(-1) = \gamma(G + E) \tag{39a}$$

$$u(1)=\gamma(G-E)+1. \tag{39b}$$

From Eq. (38), one can obtain the expression for velocity as below:

$$u(y)=-\frac{1}{G(n+1)}\left(E-Gy-\tau_y\right)^{n+1}+F \tag{40}$$

where F is the constant of integration to be determined. Using the boundary conditions Eqs. (39a) and (39b) in Eq. (40), we get

$$\left(E+G-\tau_y\right)^{n+1}+(n+1)G\gamma(G+E)-(n+1)GF=0 \tag{41a}$$

$$\left(E-G-\tau_y\right)^{n+1}+(n+1)G\left(\gamma(G-E)+1\right)-(n+1)GF=0. \tag{41b}$$

From Eqs. (41a) and (41b), one can get the following nonlinear algebraic equation in the unknown E:

$$\left\{\left(E+G-\tau_y\right)^{n+1}-\left(E-G-\tau_y\right)^{n+1}\right\}+(n+1)G(2\gamma E-1)=0. \tag{42}$$

For a given set of values of the parameters τ_y, γ, n and G, one can numerically solve the nonlinear Eq. (42) using the Newton-Raphson method. The non-dimensional flow rate per unit width of the plates is obtained with the help of Eq. (40) as below:

$$Q=\int_{-1}^{1}u(y)\,dy=\frac{\left[\left(E-G-\tau_y\right)^{n+2}-\left(E+G-\tau_y\right)^{n+2}\right]}{G^2(n+1)(n+2)}+2F. \tag{43}$$

The skin friction or wall shear stress at the lower plate and upper plate are defined respectively as

$$\tau_{LW}=\tau\big|_{y=-1}=\left\{\left(\frac{du}{dy}\right)^{1/n}\right\}_{y=-1}+\tau_y=E+G, \tag{44a}$$

$$\tau_{UW}=\tau\big|_{y=1}=\left\{\left(\frac{du}{dy}\right)^{1/n}\right\}_{y=1}+\tau_y=E-G \tag{44b}$$

where the subscripts LW and UW denote the lower wall and upper wall respectively. The frictional resistance to flow is defined as

$$\Lambda=\frac{G}{Q}. \tag{45}$$

As mentioned in the introduction section, for particular values of the parameters (yield stress τ_y and power law index n), the H-B fluid model reduces to Newtonian fluid model, power law fluid model and Bingham fluid model. For each of these reduced fluid models, the non-dimensional form of the governing equation of motion, boundary conditions, expressions for velocity, flow rate, wall shear stress and frictional resistance to flow in the (i) plane Couette flow, (ii) plane Poiseuille flow and (iii) generalized Couette flow are summarized in Appendix.

3. Numerical simulation of results

Three types of basic flows such as (i) plane Couette flow, (ii) plane Poiseuille flow and (iii) generalized Couette flow of viscous incompressible H-B fluid between parallel plates are considered in this study, treating the flow as steady, laminar and fully developed. The analytical solutions to velocity distribution, wall shear stress, flow rate and frictional resistance to flow have been obtained. The values of the arbitrary constants A, C and E appearing in these analytical solutions are found numerically, using Newton-Raphson method. The variation of these flow quantities with various physical parameters such as power law index, yield stress, slip parameter and pressure gradient are discussed in this section through appropriate graphs. Matlab program code is developed to compute the data from the analytical solutions obtained for plotting the graphs. To validate the present study, some results are com pared with that of Ramesh and Devakar [36]. The range of parameters used in this study is listed below [36, 40, 41]:

Power law index n: 0.75 - 1.5; Yield stress τ_y : 0 - 0.2; Slip parameter γ : 0 - 0.5; Pressure gradient P: 4 - 10.

3.1 Velocity distribution

Figs. 2(a)-(c) depict the velocity distribution in (i) plane coquette flow, (ii) plane Poiseuille flow and (iii) generalized Couette flow respectively, for different values of the power law index with $\gamma=0.5$, $G=10$ and $\tau_y=0.1$. In plane Couette flow, the velocity increases linearly in the y direction, whereas in plane Poiseuille flow and generalized Couette flow, parabolic velocity profiles are obtained. For a given set of values of the parameters γ, G and τ_y, the fluid velocity is marginally higher in generalized Couette flow than in plane Poiseuille flow and the fluid velocity in these flows is significantly higher than that of plane Couette flow. In the plane Couette flow, the velocity of the fluid decreases with the increase of the power law index n in the lower half of the flow region (from $y=-1$ to $y=0$) and this behavior is reversed with the increase of the power law index n in the upper half of the flow region (from $y=0$ to $y=-1$), whereas in plane Poiseuille flow and generalized Couette flow, the fluid velocity increases significantly with the increases of the power law index n.

Velocity distributions for different values of the pressure gradient in plane Poiseuille flow and generalized Couette flow are shown in Figs. 3(a) and (b), respectively. It is noticed that

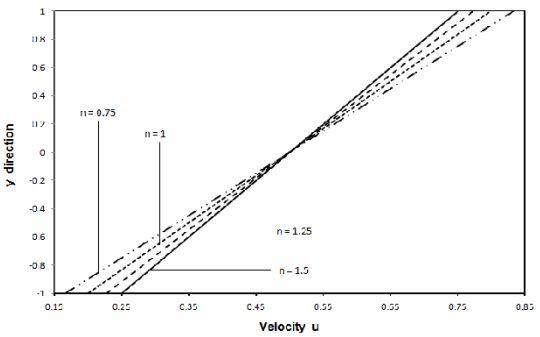

(a) Plane Couette flow

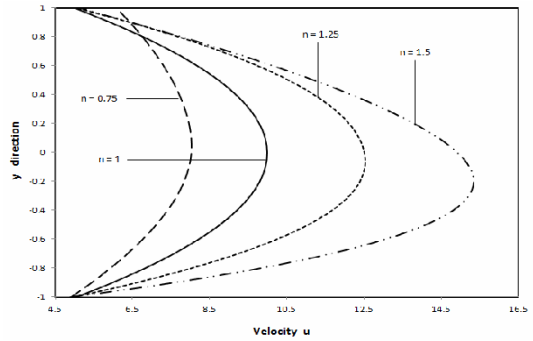

(b) Plane Poiseuille flow

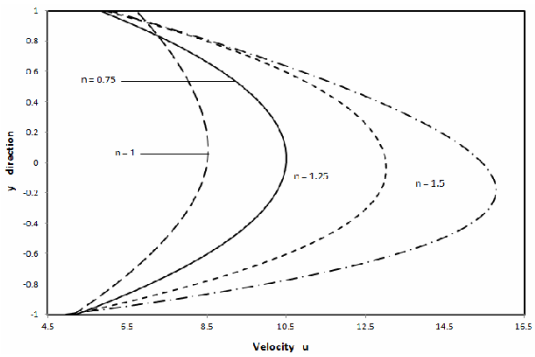

(c) Generalized Couette flow

Fig. 2. Velocity distribution for different values of power law index n with $\gamma = 0.5$, $G = 10$ and $\tau_y = 0.1$.

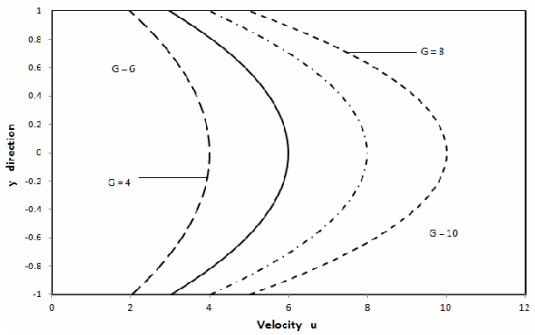

(a) Plane Poiseuille flow

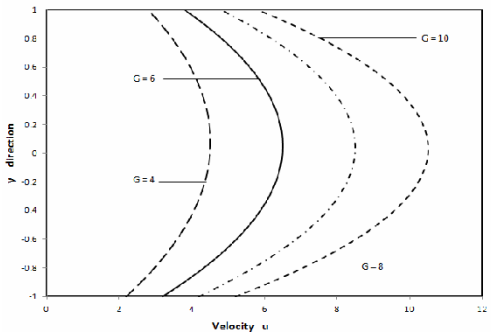

(b) Generalized Couette flow

Fig. 3. Velocity distribution for different values of pressure gradient G with with $\gamma = 0.5$, $n = 1$ and $\tau_y = 0.1$.

the fluid velocity increases significantly with the increase of the pressure gradient. Figs. 4(a)-(c) depict the velocity distribution for different values of the slip parameter γ with $n = 1$, $G = 10$ and $\tau_y = 0.1$ in (i) plane Couette flow, (ii) plane Poiseuille flow and (iii) generalized Couette flow, respectively. It is seen that the velocity of the fluid increases considerably with the increase of the slip parameter in all the types of flows. The velocity distribution for different values of the yield stress τ_y with $n = 1$, $G = 10$ and $\gamma = 0.5$ in (i) plane Couette flow, (ii) plane Poiseuille flow and (iii) generalized Couette flow sketched in Figs. 5(a)-(c), respectively. It is observed that in all the types of flows, the fluid velocity decreases very slightly with the increase of the yield stress parameter τ_y when all the other parameters are held fixed. When $\tau_y = 0$ and $n = 1$, the Herschel-Bulkley fluid model reduces to Newtonian fluid model. It is of interest to note that the velocity profiles obtained for the Newtonian fluid model in all the three types of flows are in good agreement with Figs. 5(a)-(c) of Ramesh and Devakar [35] and this validates the present study.

3.2 Flow rate

The variation of flow rate with the pressure gradient for different values of n and γ with $\tau_y = 0.1$ in plane Poiseuille flow and generalized Couette flow are shown in Figs. 6(a) and (b), respectively. It is observed that for a given set of values of

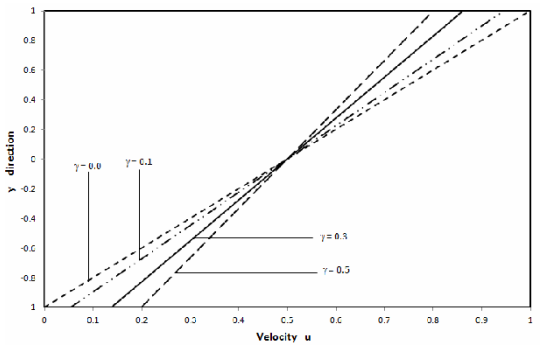

(a) Plane Couette flow

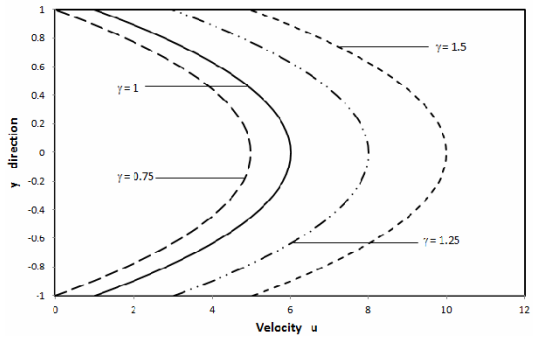

(b) Plane Poiseuille flow

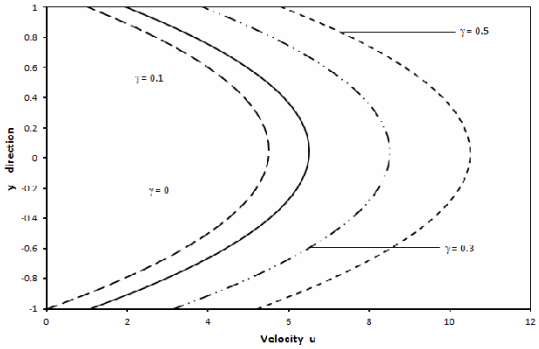

(c) Generalized Couette flow

Fig. 4. Velocity distribution for different values of slip parameter γ with $G = 10$, $n = 1$ and $\tau_y = 0.1$.

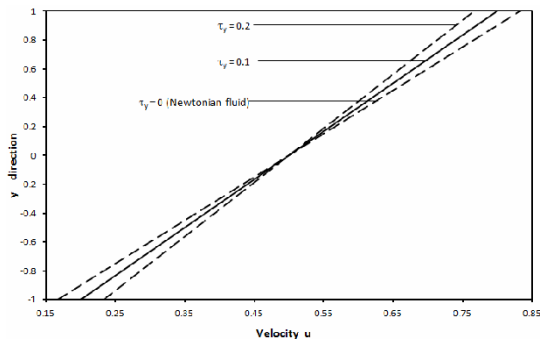

(a) Plane Couette flow

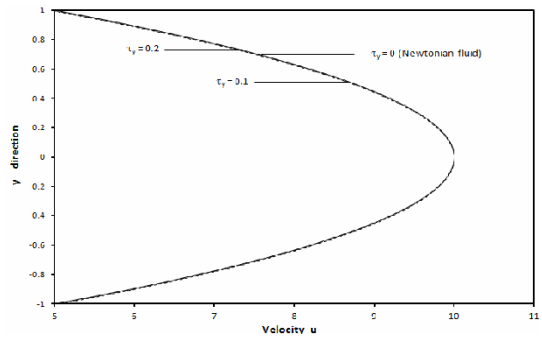

(b) Plane Poiseuille flow

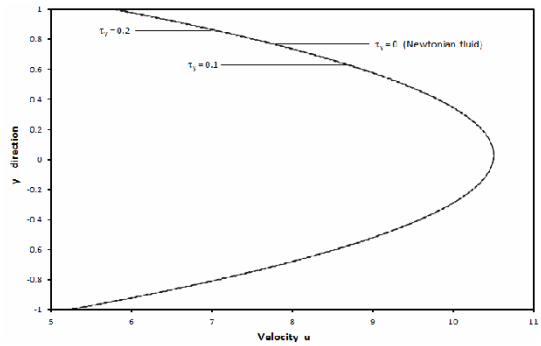

(c) Generalized Couette flow

Fig. 5. Velocity distribution for different values of yield stress τ_y with $G = 10$, $n = 1$ and $\gamma = 0.5$.

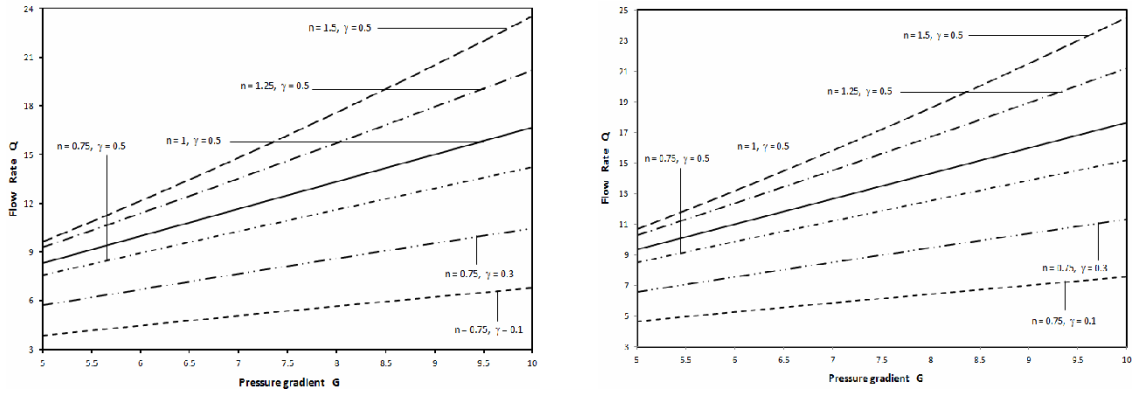

(a) Plane Poiseuille flow (b) Generalized Couette flow

Fig. 6. Variation of flow rate with pressure gradient for different values of n and γ witn $\tau_y = 0.1$.

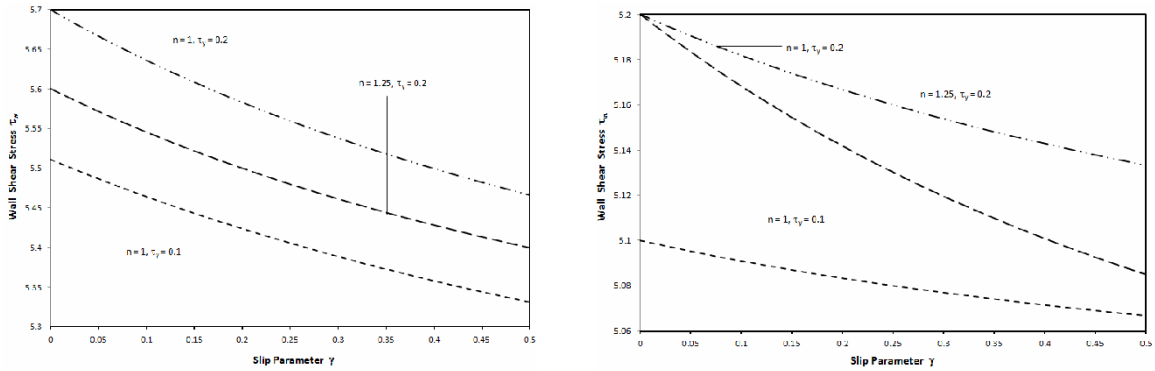

(a) Plane Poiseuille flow (b) Generalized Couette flow

Fig. 7. Variation of wall shear stress with slip parameter for different values of n and τ_y with $G = 5$.

the parameters, the flow rate of the fluid increases slowly with the increase of the pressure gradient G from 5 to 7 and then it increases linearly with the further increase of the pressure gradient from 7 to 10. One can note that the flow rate of the fluid increases considerably with the increase of either the power law index n or the slip parameter γ. It is also found that for a given set of values of the parameters, the flow rate of the fluid is marginally higher in generalized Couette flow than in plane Poiseuille flow.

3.3 Wall shear stress

The variation of wall shear stress with slip parameter γ for different values of n and τ_y with $G = 5$ in plane Poiseuille flow and generalized Couette flow are shown in Figs. 7(a) and (b). It is seen that the wall shear stress decreases rapidly with the increase of the slip parameter γ from 0 to 0.25 and then it decreases slowly with the further increase of the slip parameter γ from 0.25 to 5. It is also noticed that for a given value of the power law index n, the wall shear stress increases considerably with the increase of the yield stress τ_y of the fluid and this behavior is reversed when the power law index n increases when the yield stress τ_y is kept as constant. For a given choice of the parameters, the wall shear stress is considerably higher in plane Poiseuille flow than in generalized Couette flow.

3.4 Frictional resistance to flow

Figs. 8(a) and (b) show the variation of frictional resistance to flow with slip parameter for different values of the power law index n with $G = 10$ and $\tau_y = 0.1$ in plane Poiseuille flow and generalized Couette flow, respectively. It is seen that when the fluid is of shear thinning nature ($n \le 1$), the frictional resistance to flow decreases rapidly (nonlinearly) with the increase of the slip parameter γ from 0 to 0.25 and then it decreases slowly with the increase of the slip parameter γ from 0.25 to 0.5, whereas, if the fluid is of shear thickening nature, then the frictional resistance to flow decreases very slowly (almost constant) with the increase of the slip parameter γ. It also noted the frictional resistance to flow decreases significantly with the increase of the power law index n of the fluid when all the other parameters were kept as invariables. One can also notice that for a given set of values of the parameters, the frictional resistance to flow is marginally lower in generalized Couette flow than in plane Poiseuille flow.

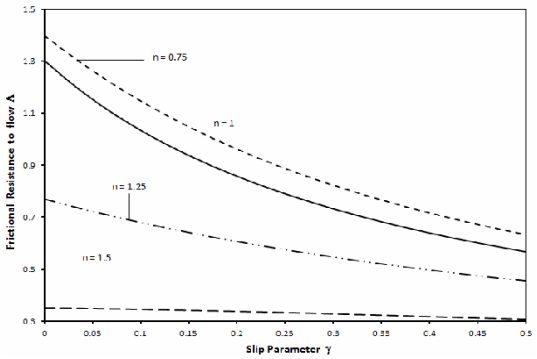

(a) Plane Poiseuille flow

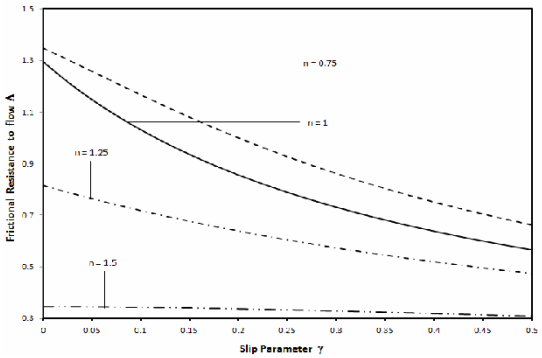

(b) Generalized Couette flow

Fig. 8. Variation of frictional resistance to flow with slip parameter for different values of power law index with $G = 10$ and $\tau_y = 0.1$.

4. Discussion

4.1 Physical significance of Herschel-Bulkley fluid model

H-B fluid is a non-Newtonian fluid model with three parameters such as the power law index, yield stress and consistency index (coefficient of viscosity). The constitutive equation of H-B fluid model which expresses the relationship between the shear stress and shear rate is defined as below:

$$\bar{\tau} = \left(-\bar{\mu}\bar{\gamma}\right)^{1/n} + \bar{\tau}_y, \tag{46}$$

where $\bar{\gamma} = d\bar{u}/d\bar{y}$ is the shear rate, $\bar{u}$ is the velocity in the horizontal direction, $\bar{\tau}$ is the shear stress in the $\bar{x}\,\bar{y}$ direction (in Cartesian plane), n is the power law index, $\bar{\mu}_H$ is the coefficient of viscosity which is shear dependent and $\bar{\tau}_y$ is the yield stress of the fluid. The shear stress of this fluid model is nonlinearly proportional to the shear rate (rate of strain/ velocity gradient). The nonlinear relationship between the shear stress and shear rate is dependent on all of the aforesaid three fluid parameters.

An advantage of using H-B fluid model for fluid flow is that the flow characteristics of the other fluid models such as Newtonian fluid model, power law fluid model and Bingham fluid model can also be obtained from H-B fluid model by assigning particular values to the fluid parameters. H-B fluid model reduces to Newtonian fluid model when $n = 1$ and $\bar{\tau}_y = 0$, Bingham fluid model when $n = 1$ and $\bar{\tau}_y \neq 0$, and power law fluid model when $n \neq 1$ and $\bar{\tau}_y = 0$. The power law index parameter n plays an important role in the major classification of non-Newtonian power law fluids. When $n < 1$, it behaves like shear thinning fluids and when $n > 1$, it exhibits the characteristics of shear thickening fluids. In shear thinning fluids, the fluid viscosity decreases with the increase of the shear stress whereas this behavior is reversed in shear thickening fluids.

Polymer solutions, molten polymers, suspensions like ketchup, whipped cream, blood, paint and nail polish are some examples of shear thinning fluids. When a modern paint is applied on a wall, the shear created by the brush or roller will allow them to thin and wet out the surface evenly. Once applied, the paints regain their higher viscosity which avoids drips and runs.

Corn starch, silica and polyethylene glycol, quicksand and dilatant fluids are some of the well known examples for shear thickening fluids. Cornstarch is a good shear thickening agent used in cooking. When a force is applied to a mixture of cornstarch and water, the cornstarch acts as a solid and resists the force.

The variation of shear stress with shear rate for different values of the coefficient of viscosity μ and yield stress τ_y for (i) $n = 0.75$, (ii) $n = 1$ and (iii) $n = 1.25$ is delineated in Figs. 9(a)-(c). Fig. 9(a) exhibits that in shear thinning fluids $(n < 1)$, the shear stress increases rapidly (nonlinearly) with the increase of the shear rate from $0\,s^{-1}$ to $0.5\,s^{-1}$ and then it increases linearly with the increase of the shear rate from $0.5\,s^{-1}$ to $1\,s^{-1}$. This trend indicates that the shear stress becomes almost constant with the further increase of the shear stress which confirms the shear thinning behavior of fluid for high shear rates.

Fig. 9(b) indicates that the shear stress increases linearly with the increase of the shear rate of the fluid when the power law index $n = 1$ which is the character of Newtonian fluid when the yield stress $\bar{\tau}_y = 0$ and Bingham fluid when the yield stress $\bar{\tau}_y \neq 0$.

Fig. 9(c) illustrates that the shear stress of the shear thickening fluid increases linearly with the increase of the shear rate from $0\,s^{-1}$ to $0.5\,s^{-1}$ and then it increases rapidly (nonlinearly) with the increase of the shear rate from $0.5\,s^{-1}$ to $1\,s^{-1}$. This trend predicts the fact that the shear stress increases very rapidly with the further increase of the shear stress which proves the shear thickening characteristic of the fluid for high shear rates. From Figs. 9(a)-(c), it is also clear that the shear stress increases considerably with the increase of the coefficient of viscosity $\bar{\mu}_H$ and yield stress $\bar{\tau}_y$ of the fluid.

The variation of shear stress with shear rate for different values of the power law index n with the yield stress $\bar{\tau}_y = 0.1$ (Poise) and viscosity coefficient $\bar{\mu}_H = 1.5$ (Poise second) is depicted in Fig. 10. One can easily understand the shear thinning and shear thickening character of H-B fluid when $n < 1$ and $n > 1$, respectively.

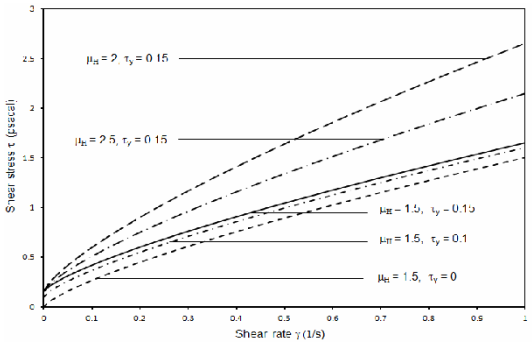

(a) $n = 0.75$

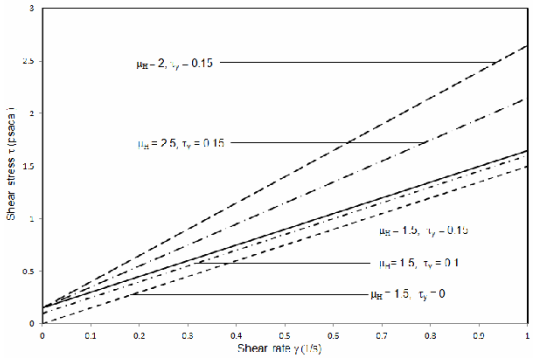

(b) $n = 1$

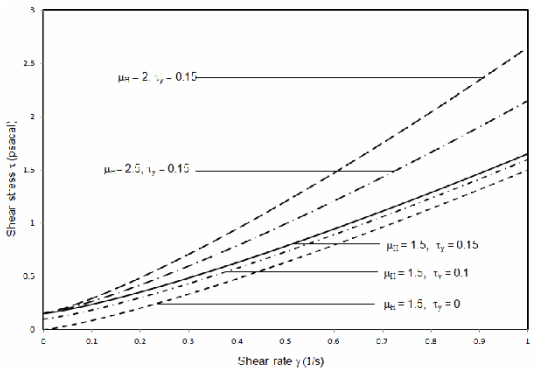

(c) $n = 1.25$

Fig. 9. Variation of shear stress with shear rate for different values of coefficient of viscosity $\overline{\mu}_H$ and yield stress $\overline{\tau}_y$ with (a) n = 0.75; (b) n = 1.0; (c) n = 1.25.

4.2 Some applications of Herschel-Bulkley fluid model

From the Refs. [1-4], it is evident that the plane Poiseuille flow, plane Couette flow and generalized Couette flow are some of the basic flow types which are widely used to understand many complex flow problems. Some physical flows of these kinds with slip at the wall are polymer extrusion process, polymer melting, gross melt fracture, sharkskin, stick-slip, bio-fluid (blood, synovial fluids, lymphatic fluids etc.) flow in clinical devices used for diagnostics [14, 42, 43]. From the above discussion, it is clear that H-B fluid model has the ability to explain these kinds of physical phenomena.

As an example, let us consider the plane Poiseuille flow

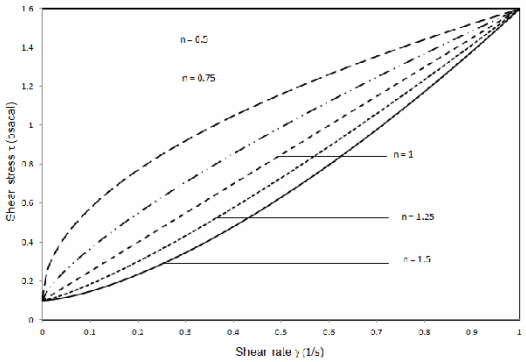

Fig. 10. Variation of shear stress with shear rate for different values of the power law index n with coefficient of viscosity $\overline{\mu}_H = 1.5$ $\left(Pascal \times \sec ond\right)$ and yield stress $\overline{\tau}_y = 0\left(Pascal\right)$.

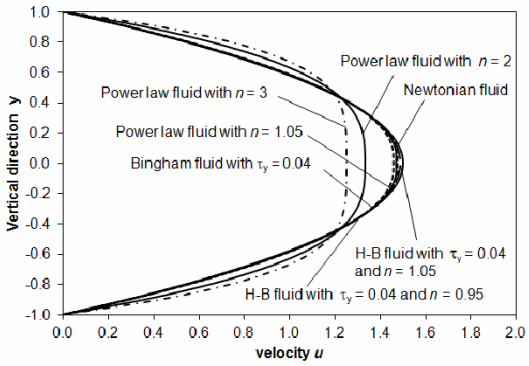

Fig. 11. Velocity distribution of Herschel-Bulkley fluid model in the plane Poiseuille flow between parallel plates for different values of the power law index n and yield stress $\overline{\tau}_y$.

(pressure driven flow) of blood (treated as viscous incompressible non-Newtonian H-B fluid) in a channel between parallel plates (clinical devises used for diagnosis of bio-fluids) which has the characteristics of laminar, axi-symmetric and fully developed unidirectional flow. Fig. 11 exhibits the velocity profiles of H-B fluid for different values of its parameters such as power law index n and yield stress $\overline{\tau}_y$. One can notice the difference between the flow patterns of the shear thinning fluid $\left(n < 1\right)$ and shear thickening fluid $\left(n > 1\right)$ and also the difference between the flow patterns of the fluids with yield stress $\left(\overline{\tau}_y \neq 0\right)$ and fluids without yield stress $\left(\overline{\tau}_y = 0\right)$. One can also realize the fact that shear thickening fluids $\left(n > 1\right)$ have the flattened parabolic velocity profile and shear thinning fluids have velocity profiles which are almost parabolic.

5. Conclusions

This mathematical analysis brings out many important and useful results in the steady, laminar and fully developed flow of viscous incompressible Herschel-Bulkley fluid between parallel plates, considering three types of flows such as (i) plane Couette flow (ii) plane Poiseuille flow and (iii) generalized coquette flow. The main findings of this theoretical inves-

tigation are summarized below:

- In plane Couette flow, the fluid velocity increases marginally with the increase of the slip parameter, power law index and decreases marginally with the increase of the power law index.
- In plane Poiseuille flow and generalized Couette flow, the velocity and flow rate of the fluid increase considerably with the increase of the slip parameter, power law index, pressure gradient.
- The fluid velocity is significantly higher in plane Poiseuille flow than in plane Couette flow.
- The wall shear stress and frictional resistance to flow of the fluid decrease considerably with the increase of the power law index n and these are increasing significantly with the increase of the yield stress of the fluid.
- The wall shear stress and frictional resistance to flow decrease rapidly with the increase of the slip parameter γ from 0 to 2.5 and then they decrease slowly with the increase of the slip parameter from 0.25 to 0.5.
- The fluid velocity and flow rate are considerably higher in generalized Couette flow than in plane Couette flow.
- The wall shear stress and frictional resistance to flow are considerably higher in plane Poiseuille flow than in generalized Couette flow.

From the recorded outcomes of this investigation, it is found that there are significant difference between the flow quantities obtained in the generalized Couette flow, plane Poiseuille flow and plane Couette flow. The present study could be applied to analyze some industrial flow problems such as polymer extrusion process and polymer melting process in which the wall slip occurs essentially. Since some physical flow through parallel plates is unsteady, the present steady flow analysis can be extended to unsteady case, this mathematical analysis would be carried out in the near future.

Acknowledgment

This study was supported by Inha University research grant.

Nomenclature

$(\bar{x},\bar{y},\bar{z})$: Cartesian coordinate system in dimensional form
(x,y,z) : Cartesian coordinate system in dimensionless form
$\vec{q}$: Velocity vector
$\bar{p}$: Fluid pressure
$\bar{J}_2$: Second invariant of the stress tensor
$\bar{V}_{ij}$: Deformation tensor
n : Power law index
$\bar{u}, u$: Axial component of velocity in dimensional and non-dimensional form
$\bar{U}$: Applied Constant velocity
$\bar{h}, h$: Semi-width of the channel in dimensional and non-dimensional form
G : Non-dimensional pressure gradient
Q : Flow rate

Greek symbols

$\bar{\rho}$: Fluid's density
$\bar{\gamma}$: Shear rate
$\bar{\sigma}_{ij}$: Cauchy's stress tensor
δ_{ij} : Kronecker delta
$\bar{\mu}$: Variable viscosity of generalized Newtonian fluid
$\bar{\mu}_H$: Viscosity coefficient of Herschel-Bulkley fluid
$\bar{\tau}_y$: Yield stress of Herschel-Bulkley fluid
τ_y : Dimensionless yield stress of Herschel-Bulkley fluid
$\bar{\beta}$: Dimensional slip parameter
γ : Dimensionless slip parameter
Λ : Frictional resistance to flow
τ_{LW} : Wall shear stress at the lower wall
τ_{UW} : Wall shear stress at the upper wall

References

[1] M. Gilbert, S. Sachin and S. Precious, Diffusion of chemically reactive species in Casson fluid flow over an unsteady stretching surface in porous medium in the presence of a magnetic field, *Mathematical Problems in Engineering*, 2015 (2015) Article Id. 724596.

[2] C. Tu and M. Deville, Pulsatile flow of non-Newtonian fluids through arterial stenosis, *Journal of Biomechanics,* 29 (7) (1996) 899-908.

[3] D. S. Sankar and U. Lee, Mathematical modeling of pulsatile flow of non-Newtonian fluid in stenosed arteries, *Communications in Nonlinear Science and Numerical Simulations,* 14 (7) (2009) 2971-2981.

[4] L. L. Ferras, J. M. Nobrega and F. T. Pinho, Analytical solutions for Newtonian and inelastic non-Newtonian flows with wall slip, *Journal of Non-Newtonian Fluid Mechanics,* 175-176 (2012) 76-88.

[5] D. S. Sankar, J. Goh and A. I. M. Ismail, FDM analysis for blood flow through stenosed tapered arteries, *Boundary Value Problems,* 2010 (2010) Article Id. 917067.

[6] N. Iida, Influence of plasma layer on steady blood flow in microvessels, *Japanese Journal of Applied Physics,* 17 (1) (1978) 203-214.

[7] C. L. M. H. Navier, *Memoires de l'Academie royale des sciences de I'Institut de France*, Royale des Scineces de l'Institut de France, 1 (1823).

[8] A. B. Basset, *A treatise on hydrodynamics,* Dover publications, New York, USA, 2 (1961).

[9] N. E. O'Neill, K. B. Ranger and H. Brenner, Slip at the surface of a translating-rotating sphere bisected by a free surface bounding a semi-infinite viscous fluid: removal of the contact-line singularity, *Physics of Fluids,* 29 (1986) 913-924.

[10] C. Tropea, A. L. Yarin and J. F. Foss, *Handbook of Experimental Fluid Dynamics,* Springer-Verlag Berlin Heidelberg, New York, USA (2007).

[11] H. Lamb, *Hydrodynamics,* Sixth Ed., Cambridge Univer-

sity Press, Cambridge, UK (1932).

[12] S. Goldstein, *Modern Developments in Fluid Dynamics: An Account of Theory and Experiment Relating to Boundary Layers, Turbulent Motion and Wakes,* Dover Publications, New York, USA, 1 (1965).

[13] G. K. Batchelor, *An Introduction to Fluid Dynamics,* Cambridge University Press, Cambridge, UK (1967).

[14] M. M. Denn, Extrusion instabilities and wall slip, *Annual Reviews of Fluid Mechanics,* 33 (1) (2001) 265-287.

[15] H. Potente, H. Ridder and R. V. Cunha, Global concept for describing and investigation of wall slip effects in the extrusion process, *Macromolecular Materials and Engineering,* 287 (11) (2002) 836-842.

[16] E. Mitsoulis, I. B. Kazatchkov and S. G. Hatzikiriakos, The effect of slip in the flow of a branched PP melt: experiments and simulations, *Rheologica Acta.*, 44 (4) (2005) 418-426.

[17] S. G. Hatzikiriakos and J. M. Dealy, Wall slip of molten high density polyethylenes, II. Capillary rheometer studies, *Journal of Rheology,* 36 (4) (1992) 703-741.

[18] X. Huang and M. H. Garcia, A Herschel-Bulkley model for mud flow down a slope, *Journal of Fluid Mechanics,* 374 (1998) 305-333.

[19] R. Ellahi, Effects of the slip boundary condition on non-Newtonian flows in a channel, *Communications in Nonlinear Science and Numerical Simulations,* 14 (4) (2009) 1377-1384.

[20] I. N. Svetlana and P. C. Clinton, The role of Poiseuille flow in creating depth-variation of asthenospheric shear, *Geophysical Journal International,* 190 (3) (2012) 1297-1310.

[21] R. Berker, Integration des equations du mouvement d'un fluide visqueux, incompressible, *Handbuch der Physik,* Springer-Verlag, Berlin, Germany (1963).

[22] R. B. Bird, C. F. Curtiss, R. C. Armstrong and O. Hassager, *Dynamics of Polymeric Liquids,* John Wiley and Sons, New York, USA, 2 (1987).

[23] S. P. Yang and K. Q. Zhu, Analytical solutions for squeeze flow of Bingham fluid with Navier slip condition, *Journal of Non-Newtonian Fluid Mechanics,* 138 (2) (2006) 173-180.

[24] M. T. Matthews and J. M. Hill, Newtonian flow with nonlinear Navier boundary condition, *Acta Mechanica,* 191 (3) (2007) 195-217.

[25] R. Ellahi, T. Hayat, F. M. Mahomed and A. Zeeshan, Fundamental flows with nonlinear slip conditions: exact solutions, *Zeitschrift fur Angewandte Mathematik und Physik*, 61 (5) (2010) 877-888.

[26] M. Chatzimina, G. Georgiou, K. Housiadas and S. G. Hatzikiriakos, Stability of the annular Poiseuille flow of a Newtonian liquid with slip along the walls, *Journal of Non-Newtonian Fluid Mechanics,* 159 (1) (2009) 1-9.

[27] H. Meijer and C. Verbraak, Modeling of extrusion with slip boundary conditions, *Polymer Engineering and Science*, 28 (11) (1988) 758-772.

[28] C. L. Roux and A. Tani, Steady solutions of the Navier-Stokes equations with threshold slip boundary conditions, *Mathematical Methods in Applied Sciences,* 30 (5) (2007) 595-624.

[29] P. Estelle and C. Lanos, Squeeze flow of Bingham fluids under slip with friction boundary conditions, *Rheologica Acta,* 46 (3) (2007) 397-404.

[30] Y. H. Wu, B. Wiwatanapataphee and M. B. Hu, Pressure-driven transient flows of Newtonian fluids through micro-tubes with slip boundary, *Physica A: Statistical Mechanics and Its Applications,* 387 (24) (2008) 5979-5990.

[31] P. A. Thompson and S. M. Troian, A general boundary condition for liquid flow at solid surfaces, *Nature*, 389 (1997) 360-362.

[32] El. Abd. Hakeem, El Abd. Naby and EI IIE Shamy, Slip effects on peristaltic transport of power law fluid through an inclined tube, *Applied Mathematical Sciences,* 1 (60) (2007) 2967-2980.

[33] Y. L. Chen and K. Q. Zhu, Couette-Poiseuille flow of Bingham fluids between two porous parallel plates with slip conditions, *Journal of Non-Newtonian Fluid Mechanics,* 153 (1) (2008) 1-11.

[34] S. Abelman, E. Momoniat and T. Hayat, Couette flow of a third grade fluid with rotating frame and slip condition, *Nonlinear Analysis: Real World Applications,* 10 (6) (2009) 3329-334.

[35] N. F. M. Noor, R. U. Haq, S. Nadeem and I. Hashim, Mixed convection stagnation flow of micropolar nanofluid along a vertically stretching surface with slip effects, *Meccanica,* 50 (2015) 2007-2022.

[36] K. Ramesh and M. Devakar, Some analytical solutions of flows of Casson fluid with slip boundary conditions, *Ain Shams Enggineering Journal*, 6 (3) (2015) 967-975.

[37] P. Chaturani and R. Ponnalagar Samy, A study of non-Newtonian aspects of blood flow through stenosed arteries and its applications in arterial diseases, *Biorheology,* 22 (6) (1985) 521-531.

[38] A. V. Mernone and J. N. Mazumdar, A mathematical study of peristaltic transport of a Casson fluid, *Mathematical and Computer Modeling,* 35 (7) (2002) 895-912.

[39] K. Vajravelu, S. Sreenadh and V. Ramesh Babu, Peristaltic transport of a Herschel-Bulkley fluid in an inclined tube, *International Journal of Non-Linear Mechanics,* 40 (1) (2005) 83-90.

[40] K. Vajravelu, S. Sreenadh and V. Ramesh Babu, Peristaltic pumping of a Herschel-Bulkley fluid in a channel, *Applied Mathematics and Computation,* 169 (1) (2005) 726-735.

[41] D. S. Sankar and M. F. Karim, Influence of body acceleration in blood flow through narrow arteries with multiple constrictions, IET Digital Library, *Proceeding of 5th Brunei Int. Conf. on Engg. and Tech*., Nov. 1-3 (2014) 1-14 (ISBN: 978-84929-991-9; Conf. No.: CP469).

[42] R. K. Dash, G. Jayaraman and K. N. Metha, Shear augmented dispersion of solute in a Casson fluid flowing in a conduit, *Annals of Biomedical Engg.,* 28 (2000) 373-385.

[43] D. S. Sankar, N. Aini and Y. Yazariah, Nonlinear analysis for shear augmented dispersion of solutes in blood flow through narrow arteries, *Journal of Applied Mathematics*,

2012, Article ID: 812535, http://dx.doi.org/10.1155/2012/812535.

Appendix

For steady, laminar and fully developed plane Couette flow of viscous incompressible (i) Newtonian fluid, (ii) power law fluid and (iii) Bingham fluid, the non-dimensional form of the governing equation of motion, boundary conditions, expressions for velocity and flow rate are obtained and are summarized in Table A.1.

In the case of plane Poiseuille flow and generalized Couette flow of these fluid models, the governing equations of motion, boundary conditions, expression for velocity, flow rate, wall shear stress and frictional resistance to flow are obtained and summarized in Tables A.2 and A.3, respectively.

Table A.1. Governing equations and the analytic solutions to plane Couette flow.

Case 1. Newtonian fluid (Reduced from H-B fluid when $\tau_y = 0$ and $n = 1$)		
Governing differential equation	$\frac{d}{dy}\left(\frac{du}{dy}\right) = 0$	(A.1)
Boundary conditions	$u(-1) - \gamma\left(\frac{du}{dy}\right)_{y=-1} = 0$	(A.2a)
	$u(1) + \gamma\left(\frac{du}{dy}\right)_{y=1} = 1$	(A.2b)
Velocity	$u(y) = \frac{1}{2}\left[1 + \frac{y}{(1+\gamma)}\right]$	(A.3)
Flow rate	$Q = 1$	(A.4)
Case 2. Power law fluid (Reduced from H-B fluid when $\tau_y = 0$)		
Governing differential equation	$\frac{d}{dy}\left(\frac{du}{dy}\right)^{1/n} = 0$	(A.5)
Boundary conditions	$u(-1) - \gamma\left[\left(\frac{du}{dy}\right)^{1/n}\right]_{y=-1} = 0$	(A.6a)
	$u(1) + \gamma\left[\left(\frac{du}{dy}\right)^{1/n}\right]_{y=1} = 1$	(A.6b)
Velocity	$u(y) = \frac{1}{2}\left[1 + (1 - 2\gamma A)y\right]$ where the value of the arbitrary constant A is obtained by solving Eq. (A.8) numerically.	(A.7)
	$2A^n + 2\gamma A - 1 = 0$	(A.8)
Flow rate	$Q = 1$	(A.9)
Case 3. Bingham fluid (Reduced from H-B fluid when $\tau_y = 0$ and $n = 1$)		
Governing differential equation	$\frac{d}{dy}\left[\left(\frac{du}{dy}\right) + \tau_y\right] = 0$	(A.10)
Boundary conditions	$u(-1) - \gamma\left[\left(\frac{du}{dy}\right) + \tau_y\right]_{y=-1} = 0$	(A.11a)
	$u(-1) + \gamma\left[\left(\frac{du}{dy}\right) + \tau_y\right]_{y=1} = 1$	(A.11b)
Velocity	$u(y) = \frac{1}{2}\left[1 + \frac{(1 - 2\gamma\tau_y)y}{(1+\gamma)}\right]$	(A.12)
Flow rate	$Q = 1$	(A.13)

Table A.2. Governing equations and the analytic solutions to plane Poiseuille flow.

Case 1. Newtonian fluid (Reduced from H-B fluid when $\tau_y = 0$ and $n = 1$)		
Governing differential equation	$\frac{d}{dy}\left(\frac{du}{dy}\right) = -G$	(A.14)
Boundary conditions	where $G = -\frac{dp}{dx}$	(A.15)
	$u(-1) - \gamma\left(\frac{du}{dy}\right)_{y=-1} = 0$	(A.16a)
	$u(1) + \gamma\left(\frac{du}{dy}\right)_{y=1} = 0$	(A.16b)
Velocity	$u(y) = -\frac{Gy^2}{2} + \frac{1}{2}(2\gamma + 1)G$	(A.17)
Flow rate	$Q = -\frac{G}{3} + (2\gamma + 1)G$	(A.18)
Wall shear stress	$\tau_{LW} = \left(\frac{du}{dy}\right)_{y=-1} = G$	(A.19a)
	$\tau_{UW} = \left(\frac{du}{dy}\right)_{y=1} = -G$	(A.19b)
Frictional resistance to flow	$\Lambda = G / Q$	(A.20)
Case 2. Power law fluid (Reduced from H-B fluid when $\tau_y = 0$)		
Governing differential equation	$\frac{d}{dy}\left(\frac{du}{dy}\right)^{1/n} = -G$	(A.21)
Boundary conditions	$u(-1) - \gamma\left[\left(\frac{du}{dy}\right)^{1/n}\right]_{y=-1} = 0$	(A.22a)
	$u(1) + \gamma\left[\left(\frac{du}{dy}\right)^{1/n}\right]_{y=1} = 0$	(A.22b)
Velocity	$u(y) = -\frac{1}{G(n+1)}(-Gy + C)^{n+1} + D$ where the value of the arbitrary constant C is obtained by solving the following Eq. (A.24) numerically	(A.23)
	$\left\{(C+G)^{n+1} - (C-G)^{n+1}\right\} + 2(n+1)\gamma GC = 0$	(A.24)

	And D is obtained form Eq. (A.25). $$D=\frac{(C-G)^{n+1}+(n+1)\gamma G(G-C)}{(n+1)G} \quad \text{(A.25)}$$
Flow rate	$$Q=\frac{(C-G)^{n+2}-(C+G)^{n+2}}{(n+1)(n+2)G^2}+2D \quad \text{(A.26)}$$
Wall shear stress	$$\tau_{LW}=\tau\big\vert_{y=-1}=\left[\left(\frac{du}{dy}\right)^{1/n}\right]_{y=-1}=C+G \quad \text{(A.27a)}$$ $$\tau_{UW}=\tau\big\vert_{y=1}=\left[\left(\frac{du}{dy}\right)^{1/n}\right]_{y=1}=C-G \quad \text{(A.27b)}$$
Frictional resistance to flow	$$\Lambda=G/Q \quad \text{(A.28)}$$

Case 3. Bingham fluid
(Reduced from H-B fluid when $\tau_y=0$ and $n=1$)

Governing differential equation	$$\frac{d}{dy}\left[\left(\frac{du}{dy}\right)+\tau_y\right]=-G \quad \text{(A.29)}$$
Boundary conditions	$$u(-1)-\gamma\left[\left(\frac{du}{dy}\right)+\tau_y\right]_{y=-1}=0 \quad \text{(A.30a)}$$ $$u(1)+\gamma\left[\left(\frac{du}{dy}\right)+\tau_y\right]_{y=1}=0 \quad \text{(A.30b)}$$
Velocity	$$u(y)=-\frac{Gy^2}{2}-\frac{\gamma\tau_y y}{(1+\gamma)}+\frac{1}{2}(1+2\gamma) \quad \text{(A.31)}$$
Flow rate	$$Q=-\frac{G}{3}+(2\gamma+1) \quad \text{(A.32)}$$
Wall shear stress	$$\tau_{LW}=\tau\big\vert_{y=-1}=\left[\left(\frac{du}{dy}\right)\right]_{y=-1}+\tau_y=\frac{\tau_y}{(2\gamma+1)}+G \quad \text{(A.33a)}$$ $$\tau_{UW}=\tau\big\vert_{y=1}=\left[\left(\frac{du}{dy}\right)\right]_{y=1}+\tau_y=\frac{\tau_y}{(2\gamma+1)}-G \quad \text{(A.33b)}$$
Frictional resistance to flow	$$\Lambda=G/Q \quad \text{(A.34)}$$

Table A.3. Governing equations and the analytic solutions to generalized Couette flow.

Case 1. Newtonian fluid
(reduced from H-B fluid when $\tau_y=0$ and $n=1$)

Governing differential equation	$$\frac{d}{dy}\left(\frac{du}{dy}\right)=-G \quad \text{(A.35)}$$
Boundary conditions	$$u(-1)-\gamma\left(\frac{du}{dy}\right)_{y=-1}=0 \quad \text{(A.36a)}$$ $$u(1)+\gamma\left(\frac{du}{dy}\right)_{y=1}=0 \quad \text{(A.36b)}$$
Velocity	$$u(y)=-\frac{Gy^2}{2}+\frac{y}{(2\gamma+1)}+\frac{(2\gamma+1)G+1}{2} \quad \text{(A.37)}$$
Flow rate	$$Q=-\frac{G}{3}+\left[(2\gamma+1)G+1\right] \quad \text{(A.38)}$$
Wall shear stress	$$\tau_{LW}=\tau\big\vert_{y=-1}=\left(\frac{du}{dy}\right)_{y=-1}=\frac{1}{(2\gamma+1)}+G \quad \text{(A.39a)}$$ $$\tau_{UW}=\tau\big\vert_{y=1}=\left(\frac{du}{dy}\right)_{y=1}=\frac{1}{(2\gamma+1)}-G \quad \text{(A.39b)}$$
Frictional resistance to flow	$$\Lambda=G/Q \quad \text{(A.40)}$$

Case 2. Power law fluid
(Reduced from H-B fluid when $\tau_y=0$)

Governing differential equation	$$\frac{d}{dy}\left(\frac{du}{dy}\right)^{1/n}=-G \quad \text{(A.41)}$$
Boundary conditions	$$u(-1)-\gamma\left[\left(\frac{du}{dy}\right)^{1/n}\right]_{y=-1}=0 \quad \text{(A.42a)}$$ $$u(1)+\gamma\left[\left(\frac{du}{dy}\right)^{1/n}\right]_{y=1}=1 \quad \text{(A.42b)}$$
Velocity	$$u(y)=-\frac{1}{G(n+1)}(-Gy+E)^{n+1}+F \quad \text{(A.43)}$$ where the value of the arbitrary constant E is obtained by solving the following equation numerically: $$\left\{(E+G)^{n+1}-(E-G)^{n+1}\right\}+(n+1)G(2\gamma E-1)=0. \quad \text{(A.44)}$$ and F is obtained from the following equation: $$F=\frac{(E+G)^{n+1}+(n+1)\gamma G(G+E)}{(n+1)G}. \quad \text{(A.45)}$$
Flow rate	$$Q=\frac{(C-G)^{n+2}-(C+G)^{n+2}}{(n+1)(n+2)G^2}+2D \quad \text{(A.46)}$$
Wall shear stress	$$\tau_{LW}=\tau\big\vert_{y=-1}=\left[\left(\frac{du}{dy}\right)^{1/n}\right]_{y=-1}=E+G \quad \text{(A.47a)}$$ $$\tau_{UW}=\tau\big\vert_{y=1}=\left[\left(\frac{du}{dy}\right)^{1/n}\right]_{y=1}=E-G \quad \text{(A.47b)}$$
Frictional resistance to flow	$$\Lambda=G/Q \quad \text{(A.48)}$$

Case 3. Bingham fluid
(Reduced from H-B fluid when $\tau_y=0$ and $n=1$)

Governing differential equation	$$\frac{d}{dy}\left[\left(\frac{du}{dy}\right)+\tau_y\right]=-G \quad \text{(A.49)}$$
Boundary conditions	$$u(-1)-\gamma\left[\left(\frac{du}{dy}\right)+\tau_y\right]_{y=-1}=0 \quad \text{(A.50a)}$$ $$u(1)+\gamma\left[\left(\frac{du}{dy}\right)+\tau_y\right]_{y=1}=1 \quad \text{(A.50b)}$$

Velocity	$u(y) = -\frac{Gy^2}{2} + \frac{(1-2\gamma\tau_y\, y)y}{2(1+\gamma)} + \frac{G(1+2\gamma)}{2} + \frac{1}{2}$	(A.51)
Flow rate	$Q = -\frac{G}{3} + G(2\gamma+1) + 1$	(A.52)
Wall shear stress	$\tau_{LW} = \tau\big\|_{y=-1} = \left[\left(\frac{du}{dy}\right)\right]_{y=-1} + \tau_y = \frac{(1+2\tau_y)}{2(1+\gamma)} + G$	(A.53a)
	$\tau_{UW} = \tau\big\|_{y=1} = \left[\left(\frac{du}{dy}\right)\right]_{y=1} + \tau_y = \frac{(1+2\tau_y)}{2(1+\gamma)} - G$	(A.53b)
Frictional resistance to flow	$\Lambda = G/Q$	(A.54)

D. S. Sankar received his B. Sc. degree in Mathematics from the University of Madras, Chennai, India in 1989. He then received his M. Sc., M. Phil. and Ph.D. degrees from Anna University, India in 1991, 1992 and 2004, respectively. Currently, he is a Professor of Engineering Mathematics Unit, Faculty of Engineering, Universiti Teknologi Brunei, Brunei. His research interest includes Mathematical Modeling, Applied Fluid Dynamics, Biomechanics, Differential Equations and Numerical Analysis.

Usik Lee received his B.S. degree in Mechanical Engineering from Yonsei University, Korea in 1979. He then received his M.S. and Ph.D. degrees in Mechanical Engineering from Stanford University, USA in 1982 and 1985, respectively. Currently, he is a professor of the Department of Mechanical Engineering, Inha University, Korea. His research interests include structural dynamics, biomechanics and computational mechanics.